Scientific paper

Compressive Stress-Strain Behavior of Small Scale Steel Fibre Reinforced High Strength Concrete Cylinders

Pradeep Bhargava[1], Umesh K. Sharma[2] and Surendra. K. Kaushik[3]

Received 16 June 2005, accepted 12 November 2005

Abstract

An experimental investigation was carried out to generate the complete stress-strain curves of steel fibre reinforced high strength concrete under axial compression. The experimental program consisted of testing 100 x 200 mm concrete cylinders. The experimental variables of the study were concrete strength levels (58.03 MPa and 76.80 MPa), volume fractions (0.5% to 2.0%) and aspect ratios (20 and 40) of flat crimped steel fibres. The effect of the mixed aspect ratio of fibres on the stress-strain behavior of steel fibre high strength concrete was also studied by blending short and long fibres. The effects of these variables on the stress-strain curves are presented and discussed. The results indicate that high strength concrete can be made to behave in a ductile manner by the addition of suitable fibres. It is concluded that short fibres are more effective in controlling early cracking, thereby enhancing the strength of the composite, whereas long fibres are more effective in providing post peak toughness. Concrete strength seemed to have an adverse effect on the deformability of fibre reinforced high strength concrete. Based on the test data obtained, a simple model is proposed to generate the complete stress-strain relationship for steel fibre reinforced high strength concrete. The proposed model has been found to give a good representation of the actual stress-strain response.

1. Introduction

The gradual development of concrete technology has promoted the use of high strength concrete. Recently, concrete strengths much higher than 60 MPa have gained acceptance in the construction industry. Higher compressive strengths, greater modulus of elasticity and substantial savings resulting from the reduction in cross sections, are all properties of high strength concrete (HSC) that appeal to designers. One of the main applications of HSC is in the lower-storey columns of tall buildings. However, high strength concrete when subjected to short term or sustained loads tends to be brittle, lacking the plastic deformation typical in normal strength concrete. This behavior of high strength concrete raises questions about the application of the material to structures, especially in seismic regions.

It is well documented now that the addition of small, closely spaced and uniformly dispersed discrete fibers to concrete substantially improves many of its engineering properties such as tensile strength, flexural strength, fracture toughness, resistance to fatigue, impact and thermal shock. Many researchers have studied the behavior of fibre-reinforced normal strength concrete under compression (Fanella and Naaman 1985, Ezeldin and Balaguru 1992, Nataraja *et al*. 1999, Shah and Naaman 1976, Hughes and Fattuhi 1971). Typical stress-strain curves of fibre reinforced concrete in compression show a marginal increase in peak stress, an appreciable increase in strain at the peak stress and substantially higher toughness, where toughness is a measure of the ability to absorb energy. However, only a few studies exist on the behavior of steel fibre reinforced high strength concrete under compression (Hsu and Hsu 1994, Mansur *et al*. 1999, Campione *et al*. 1999).

Mohammadi and Kaushik (2003) investigated the possibility of combining fibers of various lengths (mixed aspect ratio) in the normal strength concrete matrix and concluded that improvements in both peak stress and post peak toughness can be achieved under compression, which are better than those achieved if fibers with only one aspect ratio are used. Pantazopoulou and Zanganeh (2001) studied the stress-strain behavior of steel fibre reinforced concrete in axial and tri axial compression by blending short micro fibres with long steel fibres. They observed that for the given mixed content of these fibres, the addition of micro fibres increased the pre-peak stiffness, while the longer fibres improved the post-peak toughness of the composite. These studies have definitely proved the viability of a mixed aspect ratio of fibres as an attractive option for modifying the compressive behavior of the concrete matrix.

Recently some studies have been reported, where various types of fibres have been used along with lateral confining steel to improve the post peak performance of reinforced concrete columns (Foster and attard 2001, Ramesh *et al*. 2003, Paultre *et al*. 1996). It has been shown that columns cast with suitable randomly distrib-

[1]Associate Professor, Department of Civil Engineering, Indian Institute of Technology Roorkee, India.
E-mail: bhpdpfce@iitr.ernet.in
[2]Sr. Lecturer, Civil Engineering Department, National Institute of Technology Hamirpur, India.
[3]Former Professor, Department of Civil Engineering, Indian Institute of Technology Roorkee, India.

uted discrete fibres show superior performance to comparable specimens cast without fibres, particularly with respect to post failure ductility. These studies have indicated that the fibres provide indirect confinement to the concrete and could serve the same purpose as that achieved by providing lateral confining steel in reinforced concrete columns. Further, it has been shown that steel fibres coupled with a moderate amount of lateral ties could be a good alternative to the high amount of lateral confining steel required for high strength concrete columns in seismic regions. Obviously, these recent studies have shown that fibre is a potential material for structural application in high strength concrete columns.

As part of a continuing research program aimed at investigating the strength and deformability of steel fibre reinforced high strength concrete columns, the present study attempts to investigate the stress-strain behavior of steel fibre reinforced high strength concrete under unconfined axial compression. To this end the various parameters employed are strength of concrete, fibre volume fraction, aspect ratio of fibres and mixed aspect ratio of fibres. In addition, a simple model capable of predicting the complete stress-strain curve for steel fibre reinforced high strength concrete under unconfined compression is developed.

2. Research significance

The most fundamental requirement in predicting the behavior of reinforced concrete structures is the knowledge of stress-strain behavior of the constituent materials. As concrete is basically used to resist compression, the knowledge of its behavior in compression is very important. Further if the behavior of unconfined and confined concrete in uniaxial compression is known, its flexural behavior can also be predicted. Therefore, over the last few decades, a considerable volume of research has been directed towards generating the stress-strain relationships for compressed concrete both in confined and unconfined states. As the use of fibres is now being encouraged to compensate the ductility loss of high strength concrete columns, the complete stress-strain relationships of fibrous concrete are required in both confined and unconfined states in order to analyze and design such fibre reinforced concrete columns. However, only few studies that describe the stress-strain behavior of fibre reinforced high strength concrete have been reported in the literature (Hsu and Hsu 1994, Mansur *et al*. 1999, Campione *et al*. 1999). An attempt has been made in the present study to obtain experimentally a complete stress-strain curve and to develop empirical equations in terms of this measured curve for steel fibre reinforced high strength concrete in unconfined compression.

3. Experimental program

This section describes the experimental program planned for investigating the influence of various parameters of flat crimped steel fibres on the stress strain behavior of high strength concrete under axial compression.

3.1 Material properties

Two high strength concrete mixes (Mix 1 and Mix 2) were employed in the study. The materials consisted of 43 grade Ordinary Portland Cement conforming to IS: 8112-1989, natural river sand, crushed stone aggregate with a maximum size of 10 mm, tap water for mixing and curing, silica fume and a superplasticizer admixture to maintain adequate workability of the mix. Concrete Mixes 1 and 2 had respectively 28 days average cube (150 x 150 x 150 mm) compressive strengths of 68.4 and 87.5 MPa, and average cylinder (100 x 200 mm) strengths of 58.03 and 76.80 MPa, respectively. **Table 1** lists the mix proportions and 28 days compressive strengths of both mixes. The fibres used were flat crimped steel fibres with a cross section of 2 mm x 0.6 mm (equivalent diameter = 1.24 mm). Two different lengths, short (25 mm) and long (50 mm), of these fibres were used to give aspect ratios of 20 and 40 (**Fig. 1**). Their ultimate tensile strengths were 826.61 MPa and 776.20 MPa, respectively.

3.2 Mixing casting and curing

The dry cement and aggregates were mixed for 1 minute in a tilting type rotary drum laboratory mixer. The mixing was continued for 1 more minute while approximately 50% of water was added. The mixing was continued for approximately another 1 minute and after the mix became uniform the fibres were then sprinkled in

Table 1 Mix proportions.

Mix	Cement Kg/m^3	Water Kg/m^3	Coarse Aggregate Kg/m^3	Sand Kg/m^3	Silica Fume Kg/m^3	Super-plasticizer Kg/m^3	28 Days Cylinder Compressive Strength* f_c', MPa	28 Days Cube Compressive Strength* f_{ck}, MPa
Mix 1	545	169	1105	700	--	5.45	58.03	68.40
Mix 2	600	168	1055	625	50	7.5	76.80	87.50

* Average of 5 specimens.

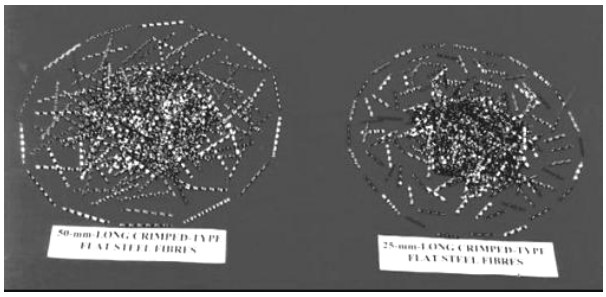

Fig. 1 Steel fibres used in the investigation.

the mixer for a period of 2 minutes. Finally, the remaining water along with the superplasticizer was added and mixing was continued for an additional 2 minutes. In the specimens where mixed aspect ratios of fibres were used, the short and long fibres were mixed together as per the desired mix proportions in a tray and then sprinkled into the mixer. A desired level of workability was achieved for both mixes at all the fibre volume fractions by using a new range water-reducing admixture (superplasticizer). It was even possible to measure the slump of fibrous concrete using a laboratory slump cone apparatus, which gave slump values ranging from 65mm to 105mm depending upon the mix type and fibre content, which seem to be quite satisfactory.

A number of different series of cylindrical specimens (100 x 200 mm) for the two mixes were cast. While it would have been preferable to use specimens with a diameter much greater than the length of the fibres, this was not possible because of the limited capacity of the testing machine. Flat crimped steel fibres at four volume fractions (0.5%, 1.0%, 1.5% and 2.0%) and two aspect ratios (20 and 40) were used to investigate the effect of these fibre parameters on high strength concrete. To study the effect of a mixed aspect ratio of fibres, the short and long fibres were blended by weight in the mix proportions of 100%-0%, 65%-35%, 50%-50%, 35%-65%, and 0%-100% respectively at 1.5% and 2.0% of fibre volume fractions to Mix 2 and at 1.5% volume fraction to Mix 1. Ideally, the shorter fibres should be short enough (micro fibres) so that they can effectively play the role of crack arrestors at the early stage of micro cracking. However, due to the non-availability of these micro fibres indigenously and based upon the encouraging results obtained from the studies reported by Gunasekaran (1975) (short fibres = 12.5 mm and long fibres = 25 mm) and Mohammadi and Kaushik (2003) (short fibres = 25 mm and long fibres = 50 mm), the present study attempts to study the effect of mixed aspect ratios of indigenous and commercially available 25 mm and 50 mm flat crimped steel fibres on high strength concrete matrix. The details of specimens with types of mix, percentage and aspect ratio of fibres investigated are given in **Table 2**. For each series, three specimens were cast in order to get the average of three results. Therefore, in all 81 specimens were cast to study the stress-strain behavior of fibrous concrete. After casting, the specimens were covered with plastic sheets and cured for 24 hours at room temperature. They were then demoulded and cured under water until testing.

3.3 Testing

All the cylindrical specimens were tested at 28 days under axial compression. Before testing, the cylinders were capped with a hard plaster to ensure parallel loading faces and constant height of the test specimens. The complete uniaxial stress-strain response of fibre reinforced concrete was obtained by testing the specimens in a 1000 kN capacity servo controlled closed loop testing machine. A slow displacement rate of loading (0.83 x 10^{-2} mm/s) was employed to capture the descending portion of the stress-strain curve. An inbuilt electronic data acquisition system of the UTM recorded the axial displacement values and the corresponding loads. The data acquisition of the UTM measured the total axial displacement over the whole length of the specimen instead of middle half-length. It was expected that this would lead to higher displacement values. Therefore, to determine the quantum of discrepancy, a compressometer with two dial gauges was fixed to the specimens at the middle 100 mm length for a limited number of test specimens to measure displacement as shown in **Fig. 2**. It was found that the average difference at the peak strain between the total strain measured over whole length between the platens of the testing machine and the strain at middle 100mm length measured by the dial gauges was of the order of 0.00066. Therefore, the displacements given directly by the data acquisition system over the entire length were used. Before testing, the specimens were loaded and unloaded twice up to 5% of the expected maximum load to take care of all loose joints and reduce as much as possible the curvilinear response, which would otherwise distort the initial portion of the stress-strain curve.

The shape of the uniaxial stress-strain curves is strongly affected by the testing conditions namely stiffness of the testing machine, size and shape of specimens, rate of loading etc. and concrete characteristics such as

Fig. 2 Test setup.

Table 2 Characteristics of specimens.

Specimen Designation	Type of Concrete Mix	Volume Fraction of Fibres V_f	Aspect Ratio of Fibres $(\frac{l_f}{d})$
LP	Mix 1	--	--
L0.5a		0.5%	20
L0.5b		0.5%	40
L1a		1.0%	20
L1b		1.0%	40
L1.5a		1.5%	20(100%) + 40(0%)
L1.5b		1.5%	20(65%) + 40(35%)
L1.5c		1.5%	20(50%) + 40(50%)
L1.5d		1.5%	20(35%) + 40(65%)
L1.5e		1.5%	20(0%) + 40(100%)
L2a		2.0%	20
L2b		2.0%	40
UP	Mix 2	--	--
U0.5a		0.5%	20
U0.5b		0.5%	40
U1a		1.0%	20
U1b		1.0%	40
U1.5a		1.5%	20(100%) + 40(0%)
U1.5b		1.5%	20(65%) + 40(35%)
U1.5c		1.5%	20(50%) + 40(50%)
U1.5d		1.5%	20(35%) + 40(65%)
U1.5e		1.5%	20(0%) + 40(100%)
U2a		2.0%	20(100%) + 40(0%)
U2b		2.0%	20(65%) + 40(35%)
U2c		2.0%	20(50%) + 40(50%)
U2d		2.0%	20(35%) + 40(65%)
U2e		2.0%	20(0%) + 40(100%)

the water/cement ratio, aggregate type etc. To minimize the effects of testing conditions, careful attention was exercised to avoid variation in the testing setup.

4. Experimental results and discussion

The specimens were tested to study the stress-strain behavior of high strength steel fibre reinforced concrete under uniaxial compression. The observed test data is presented in the form of stress-strain curves, in which the stress value is assumed to be the ratio between the load value provided by the UTM and the nominal value of the cross section of the specimen; the strain value is obtained as the mean value of the measured deformation referred to the length of the specimen. Each curve is the average of three tests. The key parameters normally used to characterize a stress-strain curve, e.g., peak stress f_{cf}', corresponding strain ε_{cf}' and the initial tangent modulus E_{if}, as obtained in this test program are presented in **Table 3**.

The energy absorbed in compression by fibre reinforced concrete, known as compressive toughness, is evaluated by the area under the stress-strain curve. A convenient way to quantify the ductility of fibre reinforced concrete is to use toughness, which is measured as either the toughness index *T.I.* or toughness ratio *T.R.* Researchers have proposed various definitions to compute *T.I.* or *T.R.* in the past (Fanella and Naaman 1985, Ezeldin and Balaguru 1992, Nataraja *et al*. 1999). In this study, the toughness is measured as toughness ratio, $T.R._{cf}$, which is the ratio of toughness of fibre reinforced concrete to that of a rigid plastic material (**Fig. 3**). Note that the toughness in each case is computed as the total area under the stress-strain curve up to a strain value of 0.015, which is sufficient to represent the trend of the post peak behavior (Fanella and Naaman 1985, Ezeldin and Balaguru 1992). Using this definition, the toughness ratios $T.R_{.cf}$ were found for all the specimens of the study and are presented in **Table 3**. To further characterize the deformability of fibre reinforced high strength concrete, a post peak strain, $\varepsilon_{0.85cf}'$, (axial strain at which the stress drops to 85% of the peak stress) was also computed for all the specimens (**Table 3**).

The discussion presented below focuses on the stress-strain behavior in compression of crimped steel fibre reinforced high strength concrete, comparing the effects of the fibre volume fraction, aspect ratio of fibre, mixed aspect ratios of fibres and concrete strength.

Table 3 Experimental and predicted results.

Specimen	R.I.		Experimental Results					Predicted Results			
	$(R.I.)_s$	$(R.I.)_l$	f_{cf}' MPa	ε_{cf}' mm/mm	E_{if} MPa	$T.R._{cf}$	$\varepsilon_{0.85cf}'$ mm/mm	f_{cf}' MPa	ε_{cf}' mm/mm	E_{if} MPa	$T.R_{cf}$
LP	0	0	57.95	0.00290	27450	0.392	0.00338	-	-	-	-
L0.5a	0.3185	0	61.78	0.00317	27468	0.447	0.00345	61.23	0.00302	27679	0.437
L0.5b	0	0.637	58.44	0.00320	27488	0.471	0.00378	59.97	0.00318	27491	0.464
L1a	0.637	0	65.80	0.003508	27690	0.53	0.00453	64.064	0.00341	27487	0.508
L1b	0	1.274	63.82	0.004115	27050	0.623	0.00538	61.550	0.00373	27111	0.582
L1.5a	0.9556	0	66.95	0.00397	27365	0.592	0.00490	66.89	0.0038	27295	0.581
L1.5b	0.6225	0.6704	65.88	0.00408	27284	0.625	0.00518	65.59	0.00397	27096	0.609
L1.5c	0.4788	0.9577	64.14	0.00425	27100	0.667	0.00612	65.02	0.00404	27011	0.621
L1.5d	0.3352	1.245	64.20	0.00433	26887	0.665	0.00745	64.45	0.00412	26926	0.634
L1.5e	0	1.915	62.87	0.00440	26769	0.714	0.00762	63.14	0.00429	26728	0.662
L2a	1.277	0	68.04	0.004561	27180	0.744	0.00765	69.753	0.00419	27101	0.673
L2b	0	2.554	64.54	0.005137	26900	0.792	0.00936	64.714	0.00483	26347	0.760
UP	0	0	75.40	0.00316	30620	0.328	0.00345	-	-	-	-
U0.5a	0.3185	0	77.02	0.00328	30860	0.38	0.00352	78.682	0.00328	30849	0.372
U0.5b	0	0.637	76.53	0.00335	30680	0.407	0.00368	77.425	0.00344	30661	0.399
U1a	0.637	0	80.13	0.003464	31050	0.41	0.00435	81.513	0.00367	30657	0.444
U1b	0	1.274	77.14	0.003999	30080	0.45	0.00490	79.000	0.00399	30281	0.498
U1.5a	0.9556	0	85.71	0.003987	30320	0.452	0.00442	84.346	0.00405	30465	0.506
U1.5b	0.6225	0.6704	84.97	0.004159	30190	0.52	0.00455	83.042	0.004232	30266	0.545
U1.5c	0.4788	0.9577	84.92	0.004325	30120	0.562	0.00496	82.474	0.00430	30181	0.557
U1.5d	0.3352	1.245	82.34	0.004387	29880	0.61	0.00579	81.908	0.00437	30096	0.569
U1.5e	0	1.915	80.56	0.004453	29650	0.604	0.00542	80.584	0.00454	29898	0.597
U2a	1.277	0	86.25	0.00444	30050	0.58	0.00528	87.203	0.00445	30271	0.589
U2b	0.83	0.894	85.85	0.004543	30100	0.598	0.00551	85.439	0.00467	30007	0.627
U2c	0.6384	1.277	85.15	0.00462	29970	0.623	0.00567	84.683	0.00477	29894	0.643
U2d	0.447	1.66	82.25	0.004718	29700	0.664	0.00646	83.928	0.00487	29781	0.659
U2e	0	2.554	81.46	0.004937	29410	0.656	0.00609	82.164	0.00509	29517	0.696

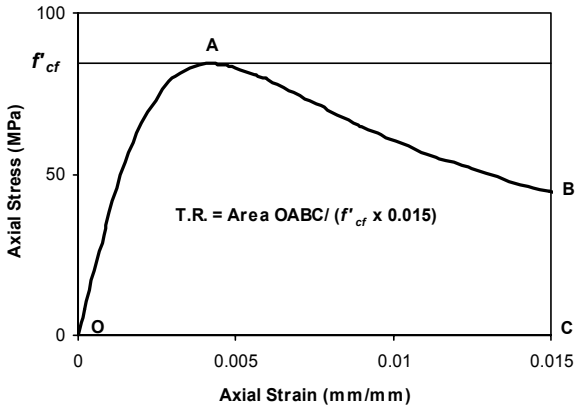

Fig. 3 Definition of toughness ratio (T.R.).

4.1 Effect of variables

The typical uniaxial compressive stress-strain curves of fibre reinforced high strength concrete showing the effect of the volume fraction and aspect ratio of fibres are given in **Figs 4** and **5** for both concrete mixes. These curves clearly show that the peak and the post peak segments of the stress-strain curve are affected extensively by the addition of fibres with almost no effect on the ascending part. A perusal of all the stress-strain curves indicated that the slope of the descending part decreases with an increase in the fibre content at a constant aspect ratio and with an increase in the aspect ratio for a constant volume fraction. It was observed that the addition of steel fibres increased the maximum strength, f_{cf}' and the corresponding peak strain, ε_{cf}' with respect to plain concrete. **Figures 6** to **9** show the percentage increase in f_{cf}' and ε_{cf}' over plain concrete (f_c' and ε_c') for both concrete mixes as the volume fraction of fibres is increased from 0.5% to 2.0% and the aspect ratio is changed from 20 (100% short fibres) to 40 (100% long fibres). It was noticed that the gain in the peak strain, ε_{cf}' was considerably more pronounced than that in the peak stress, f_{cf}'. The percentage increase in the maximum strength, f_{cf}', over plain concrete, increased from 6.6% to 17.41% and 0.84% to 11.37% with the increase in the fibre volume fraction from 0.5% to 2.0% for the specimens with 100% short fibres and 100% long fibres, respectively, for Mix 1. Similarly the percentage increase in maximum strength, f_{cf}', over plain concrete, increased from 1.34% to 13.48% and 0.7%% to 7.18% with the increase in the fibre volume fraction from 0.5% to 2.0% for the specimens with 100% short fibres and 100% long fibres respectively for

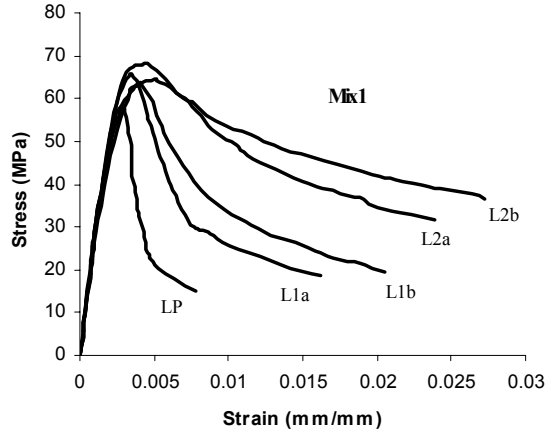

Fig. 4 Effect of volume fraction and aspect ratio of fibres for mix 1.

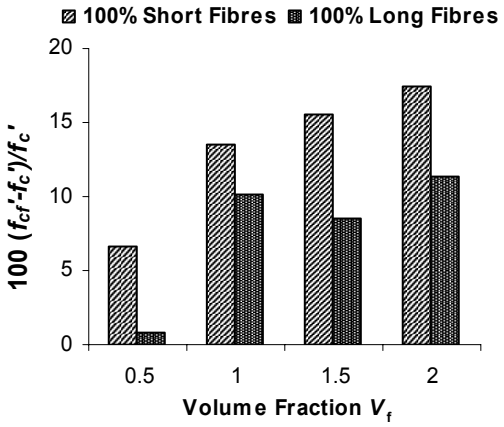

Fig. 6 % increase in peak stress v/s volume fraction of fibres at different aspect ratios for mix 1 concrete.

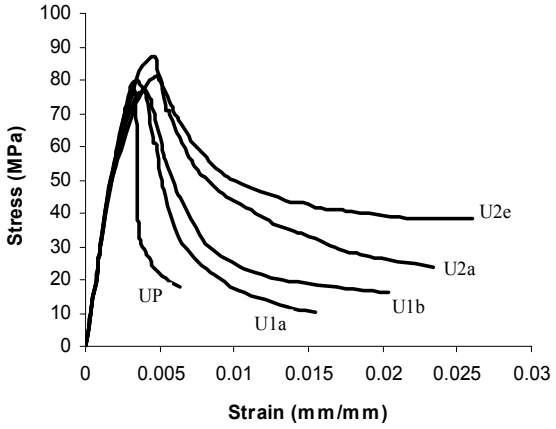

Fig. 5 Effect of volume fraction and aspect ratio of fibres for mix 2.

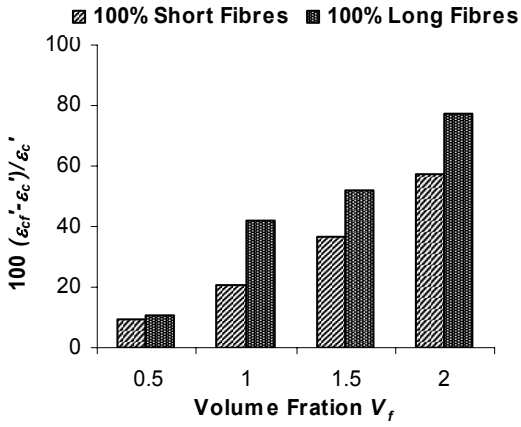

Fig. 7 % increase in peak strain v/s volume fraction of fibres at different aspect ratios for mix 1 concrete.

the higher strength mix i.e. Mix 2. This shows that the percentage increase in peak stress, f_{cf}', increased with increase in the fibre volume fraction at a constant aspect ratio, whereas it decreased slightly at the constant volume fraction with increase in the aspect ratio from 100% short fibres to 100% long fibres. This is probably due to the fact that short fibres become active earlier than longer fibres to control the initiation and propagation of initial micro-cracks. For a given volume of fibres added to the matrix, the short fibres are greater in number and therefore much closer together. Short fibres thus influence to a greater degree the early part of matrix cracking, thereby enhancing the strength of the composite as compared to longer fibres.

The percentage increase in peak strain, ε_{cf}', with respect to plain concrete increased from 9.31% to 57.27% and 10.34% to 77.14% with the fibre volume fraction (0.5% to 2.0%) for the specimens with 100% short and 100% long fibres, respectively, for Mix 1. It increased from 3.79% to 40.5% and 6.01% to 56.23%, respectively, for the specimens with 100% short and 100% long fibres for Mix 2. The percentage increase in peak strain was observed to increase with increase in fibre content for the same aspect ratio and with increase in aspect ratio for the same volume fraction of fibres, although it was more marked in the case of 100% long fibre specimens than in the case of 100% short fibre specimens. This may be due to the fact that the short fibres begin to pull out once the micro cracks start coalescing into macro cracks around the peak, thus providing lesser effect thereafter compared to longer fibres, which are now contributing to arrest these macro cracks.

The effects of volume fraction and the aspect ratio of fibres on the toughness ratio, $T.R._{cf}$, are shown in **Figs 10** and **11** for Mix 1 and Mix 2, respectively. It may be noted that the fibre volume fraction and aspect ratio of fibres markedly influence the toughness of concrete, which is a measure of ductility. In general, percentage increase in the toughness ratio, $T.R._{cf}$, with respect to that for plain concrete, $T.R._c$, increased with increase in the fibre volume fraction and aspect ratio of fibres, but concrete with fibres of a higher aspect ratio (long fibres

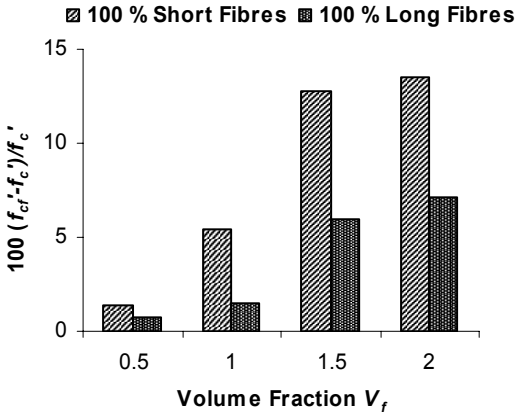

Fig. 8 % increase in peak stress v/s volume fraction of fibres at different aspect ratios for mix 2 concrete.

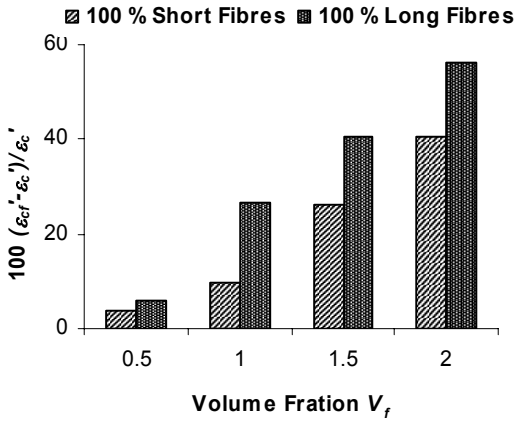

Fig. 9 % increase in peak strain v/s volume fraction of fibres at different aspect ratios for mix 2 concrete.

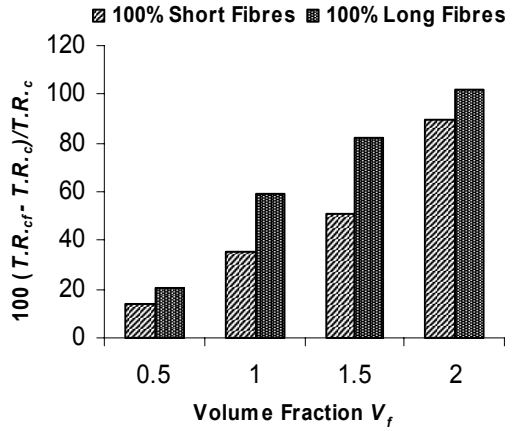

Fig. 10 % increase in toughness ratio v/s volume fraction of fibres at different aspect ratios for mix 1 concrete.

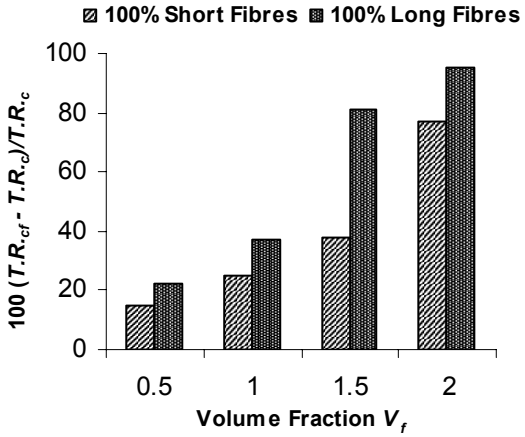

Fig. 11 % increase in toughness ratio v/s volume fraction of fibres at different aspect ratios for mix 2 concrete.

only) has greater toughness compared to concrete with fibres of a lower aspect ratio (short fibres only). This may be attributed to the fact that under increasing loads, once the cracks become quite wide in the post-peak region, the short fibres are pulled out and their structural role is relatively diminished compared to the longer fibres. The longer fibres can, however, arrest the propagation of these macro-cracks, and by their gradual pull out mode of failure, substantially improves the toughness of the composite. The percentage increase in toughness ratio, $T.R._{cf}$, was found to increase from 14.03% to 89.79% and from 20.15% to 102% with the increase in the fibre volume fraction from 0.5% to 2.0% for the concrete with 100% short and 100% long fibres respectively, for concrete Mix 1. Corresponding percentage increases in toughness ratio from 15% to 76.83% and from 22% to 94.5%, respectively, were observed for the specimens with 100% short fibres and 100% long fibres in the case of concrete Mix 2 specimens.

Similar to toughness ratio, $T.R._{cf}$, the post-peak strain, $\varepsilon_{0.85cf}'$ values also clearly show that important gains in ductility can be achieved through the introduction of fibres into the high strength concrete mix. It can be noticed that the strain $\varepsilon_{0.85cf}'$ increased with an increase in the fibre volume fraction for the same aspect ratio and with an increase in the aspect ratio for a constant fiber content. A maximum percentage increase of 177% in strain $\varepsilon_{0.85cf}'$ with respect to plain concrete was observed for the L2b specimen having 2% volume fraction of longer fibres for concrete Mix 1. On the other hand, in the case of higher strength concrete Mix 2, a maximum percentage increase of 87% was noticed in the U2d specimen having 65% of long fibres and 35% of short fibres.

The effect of mixed aspect ratio on the compressive stress-strain behavior of fibre reinforced high strength concrete was also studied by blending the long and short fibres in various proportions by weight at a constant total fibre volume fraction as described earlier. **Figures 12** and **13** show the typical experimental stress-strain curves for the different mixed aspect ratios. The per-

centage increase in peak stress, f_{cf}', and toughness ratio, $T.R._{cf}$, as compared to that for the plain concrete for various mixed aspect ratios of fibres, are schematically shown in **Figs. 14** to **16**. Based upon these results, it may be inferred that for a given total fibre content of blended fibres, as the amount of short fibres increases, the peak stress increases and the gain in toughness ratio decreases whereas, as the share of longer fibre increases the relative gain in the post peak toughness increases with a decrease in peak stress. It was observed that in the case of the U1.5d and U2.0d specimens (65% long fibres + 35% short fibres), the toughness ratios, $T.R._{cf}$, were even greater than those of the U1.5e and U2.0e specimens (100% long fibre specimens), respectively. This indicates that the combined use of short and long fibres created a better energy dissipation mechanism, the short fibres contributing at the early stage of cracking when the cracks were small in nature and the longer fibres effectively bridging the wider cracks at the later stage. Therefore, it is postulated that an advantage can be obtained using mixed aspect ratio of fibres by judiciously mixing short and long fibres to incorporate in the composite the specific advantages offered by each type of fibre.

The effect of concrete strength on the stress-strain behavior of fibre reinforced high strength concrete could be studied by comparing those specimens of Mix 1 and Mix 2, that have a similar volume fraction and aspect ratio of fibres. **Figure 17** depicts one such representative stress-strain comparison. It is interesting to observe that, the greater the strength, the greater the brittleness, because the post-peak part of the curves becomes steeper as the concrete strength increases. The results also indicated that the percentage increase in peak stress, f_{cf}', corresponding strain, ε_{cf}', and the toughness ratio, $T.R._{cf}$, over plain concrete in the case of Mix 2, i.e. the higher strength mix, were comparatively less marked compared to Mix 1, which is the lower strength mix. This suggests that Mix 2 requires more fibres to acquire the same ductility as that provided by the Mix 1 fibrous concrete. Thus, the same percentage of fibres had different effects on the behavior of two mixes with different concrete strengths.

4.2 Failure modes

The typical failure modes of some of the specimens are shown in **Fig. 18**. These failure modes were observed for plain high strength concrete and the fibre reinforced high strength concrete specimens. In the case of plain concrete cylinders the failure was due to tensile splitting and was brittle. On the other hand, when fibres were added, the mode of failure was a combination of shear failure and tensile splitting. In the case of specimens where only short fibres were present, the failure was essentially due to tensile splitting and cracks propagated parallel to the loading direction. This confirms that short fibres are mainly effective in arresting early small cracks and make a comparatively lesser contribution to

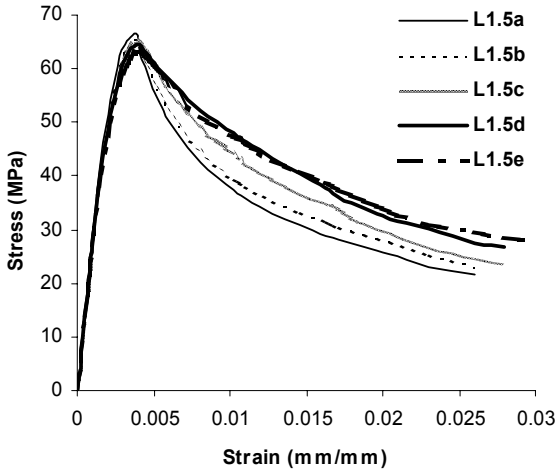

Fig. 12 Stress strain curves for mixed aspect ratio of fibres (mix 1).

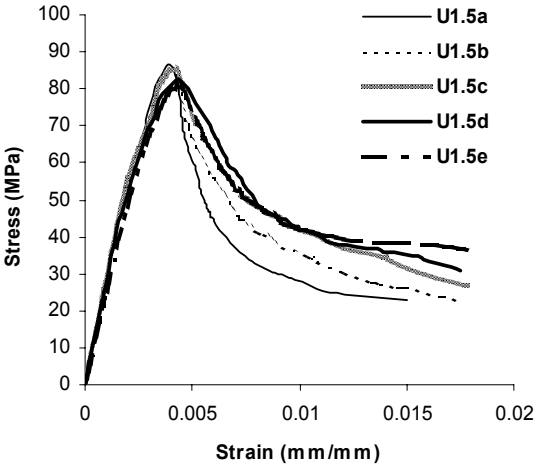

Fig. 13 Stress strain curves for mixed aspect ratio of fibres (mix 2).

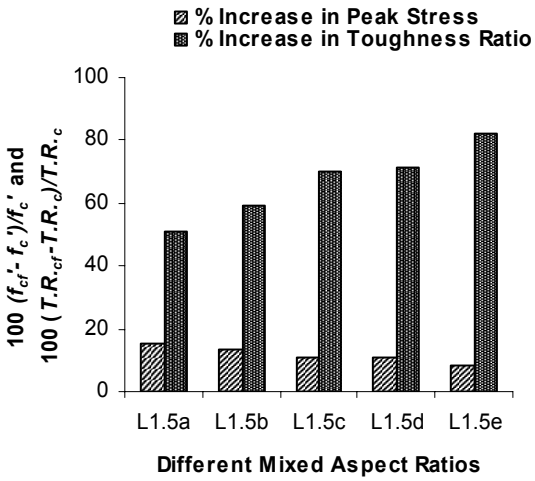

Fig. 14 % increase in peak stress and toughness ratio at different mixed aspect ratios (mix 1, Vf = 1.5%).

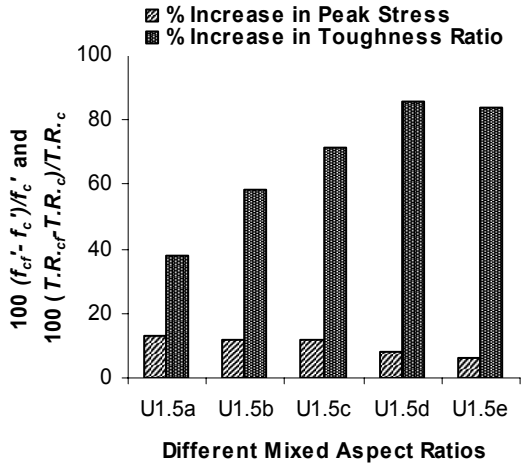

Fig. 15 % increase in peak stress and toughness ratio at different mixed aspect ratios (mix 2, Vf = 1.5%).

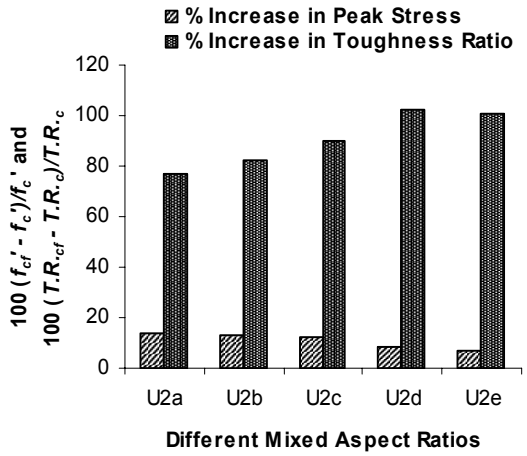

Fig. 16 % increase in peak stress and toughness ratio at different mixed aspect ratios (mix 2, Vf = 2%).

post-peak ductility. However, as the amount of long fibres increased the failure mode was marked by the bulging of the specimen in the lateral direction, with cracking along the outer surface thus, improving the ductility of the high strength concrete. **Figure 18** shows such failure modes for Mix 2 specimens in the plain state (UP) and with the addition of fibres (U1.5a, U1.5c and U1.5e). This figure clearly shows that as the amount of longer fibres increased, the failure mode changed from the tensile splitting type to the bulging type. In the case of lower high strength concrete mix (Mix 1), the same mode of failure was observed, but the behavior of the concrete was more ductile for the same fibre content and aspect ratio.

5. Analytical model

An analytical model for the complete stress-strain curve

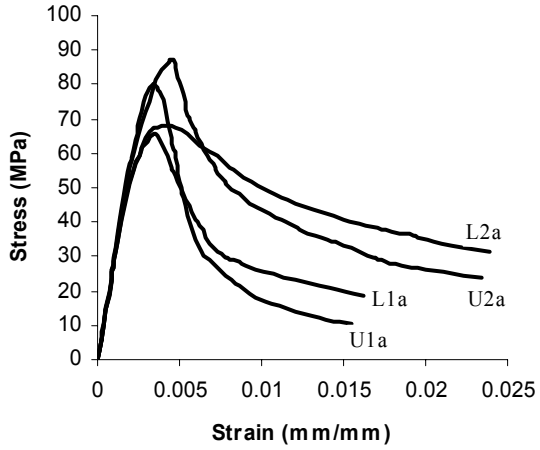

Fig. 17 Effect of concrete strength on stress-strain behavior.

of steel fibre reinforced high strength concrete is essential for the analysis and design of fibre reinforced concrete structural members. Several empirical stress-strain relationships for fibre reinforced concrete in compression have been reported in the literature (Fanella and Naaman 1985, Ezeldin and Balaguru 1992, Nataraja *et al*. 1999, Hsu and Hsu 1994, Mansur *et al*. 1999, Mohammadi and Kaushik 2003). However, most of them were developed for normal strength concrete and only a few are applicable to high strength fibrous concrete. The common parameters with physical significance used to define the stress-strain curve of fibre reinforced concrete include f_{cf}' = peak stress of fibre concrete, ε_{cf}' = strain corresponding to the peak stress f_{cf}', E_{if} = initial tangent modulus, and $R.I. = w_f(l_f / d)$ = reinforcing index of fibres by weight. After investigating various empirical expressions available in the literature, the analytical equation proposed by Carreira and Chu (1985) for plain concrete and later used by Ezeldin and Balaguru (1992) and Hsu and Hsu (1994) for steel fibrous concrete is modified here to predict the complete stress-strain curve for steel fibre reinforced high strength concrete as:

$$\frac{f_{cf}}{f_{cf}'} = \frac{k_1\beta(\frac{\varepsilon_{cf}}{\varepsilon_{cf}'})}{k_1\beta - 1 + (\frac{\varepsilon_{cf}}{\varepsilon_{cf}'})^{k_2\beta}} \quad (1)$$

$$\beta = \frac{1}{1 - \frac{f_{cf}'}{\varepsilon_{cf}' E_{if}}} \quad (2)$$

where f_{cf} and ε_{cf} = any stress and strain values on the curve, β = material parameter that, depends upon the shape of the stress-strain diagram, and k_1 and k_2 = also material parameters that depend upon the strength of the

Fig. 18 Typical failure modes.

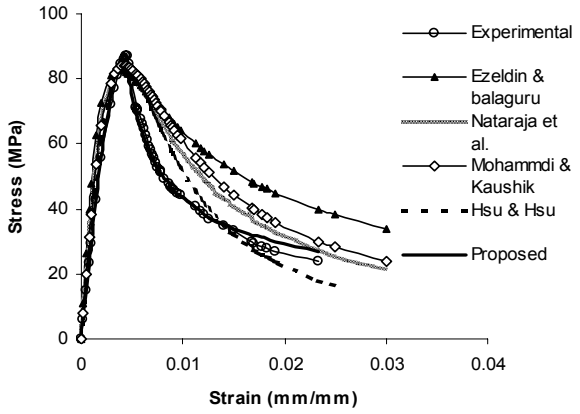

Fig. 19 Predictions by various models for L2a specimen.

material.

In the past, many researchers have used the Carreira and Chu (1985) equation to model the stress-strain behavior of fibrous concrete, but with different parameter values. A study reported by Ezeldin and Balaguru (1992) employed a similar expression to predict the stress-strain curve of hooked end steel fibre reinforced concrete. The value of a material parameter β was evaluated from the physical property of the curve, i.e. the slope of the inflection point in the descending side. Nataraja *et al*. (1999) and Mohammadi and Kaushik (2003) also used similar expressions to model the stress-strain curve of crimped steel fibre normal strength concrete and the same definition for parameter β. Hsu and Hsu (1994) modified the original Carreira and Chu (1985) expression to make it suitable for hooked end steel fibre reinforced high strength concrete. They proposed a factor *n,* which is to be multiplied by β in the numerator and denominator of the equation to properly predict the descending portion of the curve. Later, Campione (2002) also followed a similar procedure to model the stress-strain behavior of fibre reinforced high strength concrete. A comparative study of the existing stress-strain models indicated that none of the earlier models correctly predicted the descending portion of the stress-strain curves when applied to the present test data of flat crimped steel fibre high strength concrete. One such comparison is given in **Fig. 19**. Therefore, two correction factors, k_1 and k_2, are introduced in this study to correctly predict the softening branch of the stress-strain curve. The factor k_1 is applied to β values in the numerator and in the first term of the denominator, while k_2 is applied to β in the exponent of the last term of the denominator. The values of k_1 and k_2 are to be taken as unity for the ascending portion of the curve.

In stress-strain modeling of fibre reinforced concrete, the parameters of the stress-strain curve are usually related to the reinforcing index, *R.I.*, because the fibre content, length and diameter of fibres are normally known (Fanella and Naaman 1985, Ezeldin and Balaguru 1992, Nataraja *et al*. 1999). In the present study, the parameters of the proposed equation are also related to the reinforcing index, *R.I* of fibres, where $R.I. = w_f(l_f / d)$. Here w_f is the weight fraction of fibres, l_f is the length of the fibres and d is the equivalent diameter of the fibres. A best-fit statistical analysis was performed to calibrate the various parameters. In the case of a mixed aspect ratio of fibres, the *R.I.* cannot be computed by simply adding the reinforcing indices of the short and long fibres because the present study has indicated that short fibres contribute more to strength than to toughness, whereas long fibres are more effective in providing post-peak toughness. Thus, the various parameters were calibrated in terms of both the reinforcing indices of short fibres $(R.I.)_s$ and long fibres $(R.I.)_l$ to incorporate the effect of mixed aspect ratios. A non-linear multiple regression based upon the least squares method was employed to get the best fit of data points. The following lists the relationships between the parameters β, k_1, k_2, f_{cf}', ε_{cf}' and E_{if} with the reinforc-

ing indices of fibres $(R.I.)_s$, $(R.I.)_l$ and the physical parameters of plain high strength concrete. The coefficient of multiple correlation was never allowed to be less than 0.9 in deriving each of the empirical equations.

The test results showed that β is a function of peak stress of fibrous concrete and the reinforcing index of fibres. The regression analysis of the experimental results gave the following relationships for parameter β:

$$\beta = \left[\frac{f_{cf}'}{A}\right]^3 + C \tag{3}$$

where, parameters A (MPa) and C (dimensionless) are defined as:

$$A = 50.35 + 22.31(R.I.)_s + 19.13(R.I.)_l \tag{4}$$

$$C = 2.04 - 0.313(R.I.)_s - 0.155(R.I.)_l \tag{5}$$

To develop a better curve to fit the descending side of the test curves for crimped steel fibre reinforced high strength concrete, the factors k_1 and k_2 are proposed in the present analytical model. The values of these modification factors are dependent on the compressive strength, f_{cf}'. For fibre reinforced concrete, the slope of the descending portion decreases with increase in the reinforcing index of fibres. Therefore, k_1 and k_2 are related to *R.I.* of fibres also. The following expressions are proposed for the parameters based upon the regression analysis of the test data:

For the ascending portion of the curve:

$$k_1 = 1,\ k_2 = 1 \tag{6}$$

For the descending portion of the curve:

$$k_1 = \left[\frac{D}{f_{cf}'}\right]^{3.79},\ k_2 = \left[\frac{G}{f_{cf}'}\right]^{1.46} \tag{7}$$

where D (MPa) and G (MPa) are given as:

$$D = 35.635 + 17.21(R.I.)_s + 9.11(R.I.)_l \tag{8}$$

$$G = 31.82 + 16.39(R.I.)_s + 9.35(R.I.)_l \tag{9}$$

The following expressions are derived to establish relationships between the strength of fibre reinforced concrete, f_{cf}', corresponding strain, ε_{cf}', and the initial tangent modulus of fibrous concrete, E_{if}, with the corresponding parameters of plain high strength concrete:

$$f_{cf}' = f_c' + 0.45 + 8.89(R.I.)_s + 2.47(R.I.)_l \tag{10}$$

$$\varepsilon_{cf}' = \varepsilon_c' - 0.00026 + 0.001214(R.I.)_s + 0.00086(R.I.)_l \tag{11}$$

$$E_{if} = E_i + 422 - 603(R.I)_s - 597((R.I.)_l \tag{12}$$

where, f_c' = strength of plain concrete, ε_c' =strain corresponding to maximum strength f_c' of plain concrete , and E_i = initial tangent modulus of plain concrete. A regression analysis was also carried out to propose a relationship for toughness ratio $T.R._{cf}$ of crimped steel fibre reinforced high strength concrete based on the present test results. The following expression was developed for $T.R._{cf}$:

$$T.R._{cf} = T.R._c - 0.027 + 0.226(R.I.)_s + 0.155(R.I.)_l \tag{13}$$

where $T.R._c$ is the toughness ratio of plain high strength concrete. Knowing the parameters of plain high strength concrete and the reinforcing indices of short $(R.I.)_s$ and long $(R.I.)_l$ fibres, all the parameters of the proposed expression for the stress-strain curve of fibrous concrete can be estimated using expressions (3) to (11). The values of these parameters are then inserted in equation (1) to generate the complete stress-strain curve of crimped steel fibre reinforced high strength concrete. **Figure 20**

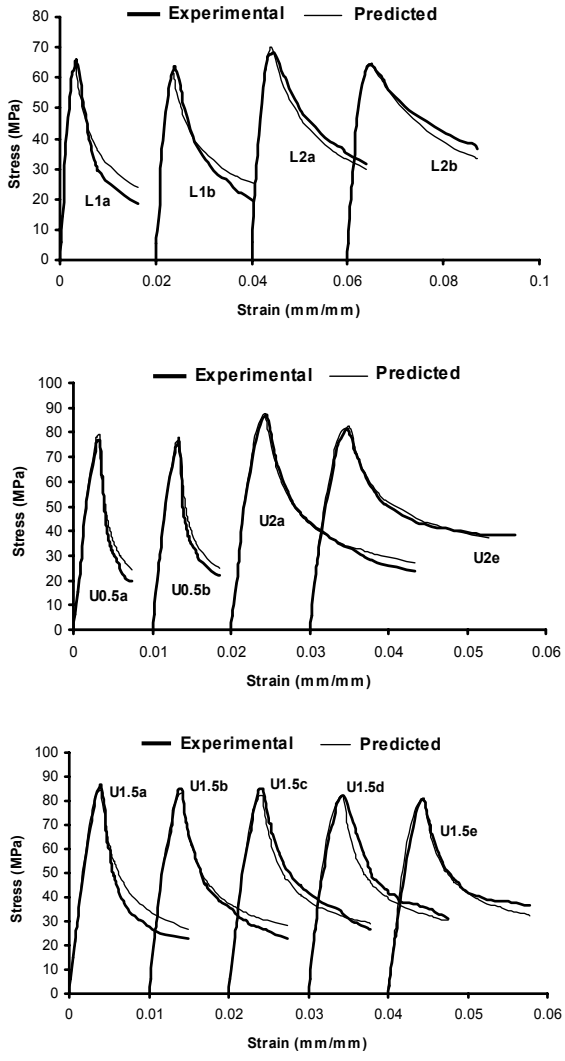

Fig. 20 Comparison of experimental and predicted curves for some of the specimens.

shows a comparison of the experimental and the analytical stress-strain curves for a few representative cases. The predictions of the proposed model can be seen to be in very good agreement with the experimental curves. A similar agreement may be noted between the experimental and the analytically found values of f_{cf}', ε_{cf}', E_{if} and $T.R._{cf}$ as summarized in **Table 3**.

6. Summary and conclusions

A total of 81 cylindrical specimens (100 x 200mm) were tested in this study to generate the complete stress-strain curves of flat crimped steel fibre reinforced high strength concrete under compression. From the test data presented and discussed here, the following conclusions may be made.

The addition of steel fibres to high strength concrete changes the basic characteristics of its stress-strain behavior. Compared with plain concrete, the ascending portion of the stress-strain curve changes slightly, but the descending portion changes remarkably. The slope of the descending part decreases with an increase in the fibre content at a constant aspect ratio and with an increase in the aspect ratio for a constant volume fraction of fibres. The gain in the peak stress, f_{cf}', over plain concrete increases with an increase in the fibre volume fraction at a constant aspect ratio, whereas it decreases for a constant volume fraction with an increase in the aspect ratio. While, both the peak strain, ε_{cf}', and toughness ratio, $T.R._{cf}$ increase with increases in the fibre content and aspect ratio of fibres, their percentage gains with reference to plain concrete are more marked in the case of longer fibres. It is concluded that short fibres are more effective in controlling early cracking, thereby enhancing the strength of the composite, while long fibres are more effective in providing post peak toughness.

It was observed that if the fibres of two different lengths, i.e. short and long fibres, are blended together at some optimum mix proportions by weight for the given total fibre content, better overall performance in terms of crack arresting capability, strength of the composite and post-peak toughness of fibrous concrete can be achieved compared to the case of a single aspect ratio. It is also concluded that the improvements in strength and ductility of concrete due to the addition of fibres decrease as the strength of concrete increases. Therefore, it can be concluded that high strength concrete requires an increased quantity of fibres to achieve the same ductility as that provided by a certain amount of fibres in the case of normal strength concrete. The study shows that the failure mode of high strength concrete is improved from tensile splitting to lateral bulging by the addition of fibres.

Analytical expressions have been proposed to predict the complete stress-strain curve of crimped steel fibre reinforced high strength concrete under unconfined compression, and good agreement has been achieved between the predicted and the experimental stress-strain curves.

References

Campione, G., Mindess, S. and Zingone, G. (1999). "Compressive stress-strain behavior of normal and high strength carbon fibre concrete reinforced with spirals." *ACI Materials Journal*, 96 (1), 27-34.

Campione, G. (2002). "The effects of fibers on the confinement models of concrete columns." *Canadian Journal of Civil Engineering*, 29, 742-750.

Carreira, D. J. and Chu, K. H. (1985). "Stress-strain relationship for plain concrete in compression." *ACI Journal*, 68 (6), 797-804.

Ezeldin, A. S. and Balaguru, P. N. (1992). "Normal and high strength fibre reinforced concrete under compression." *Journal of Materials in Civil Engineering*, 4 (4), 415-429.

Fanella, D. A. and Naaman, A. E. (1985). "Stress-strain properties of fibre reinforced mortar in compression." *ACI Journal*, 82 (4), 475-483.

Foster, S. J. and Attard, M. M. (2001). "Strength and ductility of fiber reinforced high strength concrete columns." *ASCE Journal of Structural Engineering*, 127 (1), 28-34.

Gunasekran, M. (1975). "The strength and behavior of lightweight concrete reinforced with metallic fibres of mixed aspect ratios." *Indian Concrete Journal*, 49 (2), 48-55.

Hsu, L. S. and Hsu, C. T. (1994). "Stress-strain behavior of steel fiber high strength concrete under compression." *ACI Structural Journal*, 91 (4), 448-457.

Hughes, B. P. and Fattuhi, N. I. (1977). "Stress strain curves for fibre reinforced concrete in compression." *J Cement and Concrete Research*, 7 (2), 173-183.

Mansur, M. A., Chin, M. S. and Wee, T. H. (1999). "Stress-strain relationship of high strength fibre concrete in compression." *Journal of Materials in Civil Engineering*, 11 (1), 21-29.

Mohammadi, Y. and Kaushik, S. K. (2003). "Investigations of mechanical properties of steel fibre reinforced concrete with mixed aspect ratio of fibres." *Journal of Ferrocement*, 33 (1), 1-14.

Nataraja, M. C., Dhang, N. and Gupta, A. P. (1999). "Stress-strain curves for steel fiber reinforced concrete under compression." *Journal of Cement and Concrete Composites*, 21, 383-390.

Pantazopoulou, S. J. and Zanganeh, M. (2001). "Triaxial tests of fiber reinforced concrete." *ASCE Journal of Materials in Civil Engineering*, 13 (5), 340-348.

Paultre, P., Khayat, K. H., Langlois, Y., Trundel, A. and Cusson, D. (1996). "Structural performance of some special concretes." *4th International Symposium on Utilization of High Strength/High Performance Concrete*, Paris, ENPC, 787-796.

Ramesh, K., Seshu, D. R. and Prabhakar, M. (2003). "Constitutive behavior of confined fibre reinforced

concrete under axial compression." *Journal of Cement and Concrete Composites*, 25, 343-350.

Shah, S. P. and Naaman, A. E. (1976). "Mechanical properties of glass and steel fibre reinforced mortar." *ACI Journal Proceedings*, 89 (1), 50-55.